Progress In Electromagnetics Research, Vol. 143, 447–461, 2013

SPECTRAL-DOMAIN FORMULATION OF PILLAR-TYPE PHOTONIC CRYSTAL WAVEGUIDE DEVICES OF INFINITE EXTENT

Yoshimasa Nakatake[1] and Koki Watanabe[2, *]

[1]Graduate School of Engineering, Fukuoka Institute of Technology, 3-30-1 Wajiro-Higashi, Higashi-ku, Fukuoka 811-0295, Japan

[2]Department of Information and Communication Engineering, Fukuoka Institute of Technology, 3-30-1 Wajiro-Higashi, Higashi-ku, Fukuoka 811-0295, Japan

Abstract—This paper presents a novel formulation for the modeling of electromagnetic wave propagation in pillar-type photonic crystal waveguide devices. The structure under consideration is formed in an infinitely extended pillar-type photonic crystal and the wave propagation is controlled by removing some cylinders from the original periodic structure. The structure is considered as cascade connections of straight waveguides, and the input/output properties of the devices are obtained using an analysis method of multilayer structure. Each layer includes periodic circular cylinder array with defects, and the transfer-matrix is obtained by using a spectral-domain approach based on the recursive transition-matrix algorithm with the lattice sums technique and the pseudo-periodic Fourier transform.

1. INTRODUCTION

Photonic crystal is a periodic structure consisting of high contrast dielectrics, in which the electromagnetic wave cannot transmit in a specific wavelength range. It is therefore known that, if localized defects are introduced in the photonic crystal, the electromagnetic fields are strongly confined around the defects. For example, point defects in the photonic crystal work as resonance cavities and line defects work as waveguides. Appropriate arrangements of the defects function as photonic crystal waveguide devices (PCWD), such as resonator filter, splitter, coupler, etc.

Received 14 October 2013, Accepted 18 November 2013, Scheduled 21 November 2013
* Corresponding author: Koki Watanabe (koki@fit.ac.jp).

The electromagnetic wave propagation in the PCWD has been simulated using various numerical methods such as the beam propagation method [1], the finite difference time domain method [2], and the plane wave expansion method [3]. These methods require adequate treatments of terminating conditions for the waves at the input/output ends of the circuits, which are given by straight photonic crystal waveguide (PCW) in many cases. The structure of straight PCW is periodic in the propagation direction, and the Floquet-mode analysis is necessary to decompose the fields in input/output PCWs into the forward and the backward propagating components. The Floquet-modes are the eigenmodes in periodic structures, and the Floquet theorem asserts that the fields in the structure can be expressed by superposition of the Floquet-modes [4]. Since each Floquet-mode has a pseudo-periodic property, several papers [5–7] introduce the generalized Fourier series expansion to express the fields and the dispersion equation is derived by the multilayer technique for periodic structures [8]. These approaches make us possible to obtain the guided Floquet-modes in very high accuracy, but they do not seem to be applicable to obtain the evanescent ones.

Consideration of the evanescent Floquet-modes is possible by the Fourier series expansion method (FSEM), which was originally developed to analyze the discontinuities in dielectric waveguides [9–11]. This method assumes that the fields are well confined near the defects, and introduce artificial boundaries with periodicity conditions. Then the fields are expressed in the Fourier series expansion. The field coefficients are matched at the boundary between the segments, and the input/output properties of the composite structure are obtained by the recursive calculation for stacked straight PCW sections. The FSEM was applied to the analyses of PCWs and the Floquet-modes are obtained by the eigenvalue analysis of the transfer matrix for one periodicity cell in the propagation direction [12–15]. For the PCWD formed by circular cylinders, the FSEM was combined with the recursive transition-matrix algorithm (RTMA) [16], which was originally developed to analyze the scattering problem of plural cylinders situated parallel to each other [17].

This paper considers the wave propagation in infinitely extended PCWDs formed by circular cylinders. The wave propagation is controlled by removing some cylinders from the periodic photonic crystal. As written above, the Floquet-modes of PCW can be obtained by the eigenvalue analysis of the transfer matrix for one periodicity cell in the propagation direction. The cell includes periodic circular cylinder array with defects, and the fields have continuous spectra in the wavenumber space. The FSEM discretizes the fields in the wavenumber space by introducing the periodic boundary conditions, and the transfer matrix is defined between the Fourier coefficients. The present formulation does not introduce the periodic boundary conditions, but uses the pseudo-periodic Fourier transform (PPFT) [18]. Let $f(x)$ be a function of x, and d be a positive real constant. The PPFT and its inverse are formally given by

$$\bar{f}(x;\xi) = \sum_{m=-\infty}^{\infty} f(x-md)e^{imd\xi}, \quad f(x) = \frac{1}{k_d}\int_{-k_d/2}^{k_d/2} \bar{f}(x;\xi)d\xi \tag{1}$$

where ξ is a transform parameter, and $k_d = 2\pi/d$. The transformed function $\bar{f}(x;\xi)$ has a pseudo-periodic property with the pseudo-period d in terms of x: $\bar{f}(x-md;\xi) = \bar{f}(x;\xi)\exp(-imd\xi)$ for any integer m. Also, $\bar{f}(x;\xi)$ has a periodic property with the period k_d in terms of ξ: $\bar{f}(x;\xi - mk_d) = \bar{f}(x;\xi)$ for any integer m. The transform parameter ξ relates to the wavenumber when x is the spatial parameter. If the constant d is chosen to be equal with the fundamental period in the x-direction, k_d becomes the inverse lattice constant. Because of the pseudo-periodicity of the transformed fields, the conventional grating theory based on the Floquet theorem becomes possible to be applied for the scattering problem of imperfectly periodic structures. Recently, Watanabe et al. [19] considered the scattering from periodic circular cylinder array in which some cylinders are removed, and proposed a formulation based on the RTMA with the lattice sums technique and the PPFT. The present formulation extends their approach to the analysis of wave propagation in infinitely extended PCWD formed by circular cylinders.

2. SETTING OF THE PROBLEM

This paper considers the electromagnetic wave propagation in a PCWD schematically shown in Figure 1. The structure consists of identical circular cylinders that are infinitely long and described by the radius a, the permittivity ε_c, and the permeability μ_c. The cylinders are situated in a surrounding medium with the permittivity ε_s and the permeability μ_s. The cylinder axes parallel to the z-axis are located at $(x, y) = (nd, (q-1/2)h)$ for any integer n, q, though some cylinders are removed to control the wave propagation. To indicate the removed cylinders, we introduce a notation $\mathscr{D}^{(q)}$, which is a finite subset of the integer set $\mathbb{Z}$. If an integer n is an element of $\mathscr{D}^{(q)}$, the cylinder whose center is at $(x, y) = (nd, (q-1/2)h)$ is removed.

The structure under consideration is divided into three sections by two planes $y = 0$ and $y = Q\,h$. The regions $y < 0$ and $y > Q\,h$ are

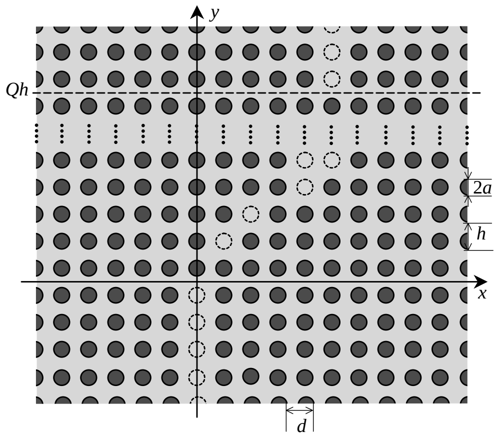

Figure 1. Geometry under consideration.

the input/output sections consisting of straight PCWs, while the other region $0 \leq y \leq Q\,h$ is a transition section. The transition section is composed of Q layers stacked in the y-direction, and arbitrary cylinders can be removed. The fields are supposed to be uniform in the z-direction. Then, the problem becomes two-dimensional, and the fields are decomposed into the transverse magnetic (TM) and the transverse electric (TE) polarizations, in which the magnetic and the electric fields are perpendicular to the z-axis, respectively. We consider time-harmonic electromagnetic fields assuming a time-dependence in $e^{-i\omega t}$. The wavenumber and the characteristic impedance in each medium are respectively denoted by $k_r = \omega\sqrt{\varepsilon_r \mu_r}$ and $\zeta_r = \sqrt{\mu_r/\varepsilon_r}$ for $r = c,\, s$.

3. OUTLINE OF FORMULATION

3.1. Transfer Matrix for Each Layer

The structure is here treated as a multilayer structure, in which periodic circular cylinder arrays with defects are stacked. The qth-layer ($q \in \mathbb{Z}$) is bounded by two planes $y = qh$ and $y = (q-1)h$. The incident field for qth-layer consists of the waves propagating in the negative y-direction from the plane $y = qh$ and the waves propagating in the positive y-direction from the plane $y = (q-1)h$. Therefore, the incident field transformed by the PPFT $\bar{\psi}^{(i)}(x;\xi,y)$ can be expressed in the plane-wave expansion [18] as

$$\bar{\psi}^{(i)}(x;\xi,y) = \mathbf{f}^{(-)}(x, y-qh;\xi)^t \bar{\boldsymbol{\psi}}^{(-)}(\xi, qh)$$

$$+\mathbf{f}^{(+)}(x, y-(q-1)h; \xi)^t \bar{\boldsymbol{\psi}}^{(+)}(\xi, (q-1)h) \tag{2}$$

where the column matrices $\mathbf{f}^{(\pm)}(x, y; \xi)$ are generated by the plane-waves whose nth-components are given by

$$\left(\mathbf{f}^{(\pm)}(x, y; \xi)\right)_n = e^{i(\alpha_n(\xi)x \pm \beta_n(\xi)y)} \tag{3}$$

with

$$\alpha_n(\xi) = \xi + nk_d, \quad \beta_n(\xi) = \sqrt{{k_s}^2 - \alpha_n(\xi)^2}. \tag{4}$$

$\bar{\boldsymbol{\psi}}^{(+)}(\xi, y')$ and $\bar{\boldsymbol{\psi}}^{(-)}(\xi, y')$ denote the column matrices of the amplitudes at $y = y'$, which correspond to the plane-waves propagating in the positive and the negative y-direction, respectively.

The formulation shown in Ref. [19] is based on RTMA, and the cylindrical-wave expansions are also used to express the fields outside the cylinders. The bases functions are given by column matrices $\mathbf{g}^{(Z)}(x, y)$ whose nth-components are expressed as

$$\left(\mathbf{g}^{(Z)}(x, y)\right)_n = Z_n(k_s\rho(x, y))e^{in\phi(x,y)} \tag{5}$$

with

$$\rho(x, y) = \sqrt{x^2 + y^2}, \quad \phi(x, y) = \arg(x + iy) \tag{6}$$

where Z specifies the cylindrical functions associating to the cylindrical-wave bases in such a way that $Z = J$ denotes the Bessel function and $Z = H^{(1)}$ denotes the Hankel function of the first kind.

Using the transform relations of the expansion bases shown in Ref. [18], Eq. (2) yields

$$\bar{\psi}^{(i)}(x; \xi, y) = \mathbf{g}^{(J)}(x, y-(q-1/2)h)^t \bar{\mathbf{a}}^{(i)}(\xi) \tag{7}$$

where the expansion coefficient matrix $\bar{\mathbf{a}}^{(i)}(\xi)$ is given by

$$\begin{aligned} \bar{\mathbf{a}}^{(i)}(\xi) = {} & \mathbf{A}^{(-)}(\xi)^t \mathbf{V}(h/2; \xi) \bar{\boldsymbol{\psi}}^{(-)}(\xi, qh) \\ & + \mathbf{A}^{(+)}(\xi)^t \mathbf{V}(h/2; \xi) \bar{\boldsymbol{\psi}}^{(+)}(\xi, (q-1)h) \end{aligned} \tag{8}$$

with

$$(\mathbf{V}(y; \xi))_{n,m} = \delta_{n,m} e^{i\beta_n(\xi)y} \tag{9}$$

$$\left(\mathbf{A}^{(\pm)}(\xi)\right)_{n,m} = \left(\frac{i\alpha_n(\xi) \pm \beta_n(\xi)}{k_s}\right)^m. \tag{10}$$

On the other hand, the scattered field consists of the outward propagating waves from the cylinders in the qth-layer, and the transformed field is expressed as

$$\bar{\psi}^{(s)}(x; \xi, y) = \sum_{n \in \mathbb{Z}} \mathbf{g}^{(H^{(1)})}(x - nd, y-(q-1/2)h)^t \bar{\mathbf{a}}^{(s)}(\xi) e^{ind\xi} \tag{11}$$

where $\bar{\mathbf{a}}^{(s)}(\xi)$ denotes the column matrix generated by the expansion coefficients of the transformed scattered field. The total fields near $y = qh$ and $y = (q-1)h$ are expressed in the plane-wave expansions with the use of the transform relations shown in Ref. [18] and the amplitude matrices corresponding to the outward propagating plane-waves as follows:

$$\bar{\boldsymbol{\psi}}^{(+)}(\xi, qh) = \mathbf{V}(h;\xi)\bar{\boldsymbol{\psi}}^{(+)}(\xi, (q-1)h) + \mathbf{V}(h/2;\xi)\mathbf{B}^{(+)}(\xi)^t\bar{\mathbf{a}}^{(s)}(\xi) \quad (12)$$

$$\bar{\boldsymbol{\psi}}^{(-)}(\xi,(q-1)h) = \mathbf{V}(h;\xi)\bar{\boldsymbol{\psi}}^{(-)}(\xi, qh) + \mathbf{V}(h/2;\xi)\mathbf{B}^{(-)}(\xi)^t\bar{\mathbf{a}}^{(s)}(\xi) \quad (13)$$

with

$$\left(\mathbf{B}^{(\pm)}(\xi)\right)_{n,m} = \frac{2}{d\beta_m(\xi)}\left(\frac{-i\alpha_m(\xi) \pm \beta_m(\xi)}{k_s}\right)^n. \quad (14)$$

An appropriate discretization is introduced in the transform parameter ξ. Considering the periodicity of the transformed functions, we take L sample points $\{\xi_l\}_{l=1}^L$ in the Brillouin zone $-k_d/2 < \xi < k_d/2$. Then, the column matrices $\bar{\mathbf{a}}^{(i)}(\xi)$, $\bar{\boldsymbol{\psi}}^{(+)}(\xi; qh)$, and $\bar{\boldsymbol{\psi}}^{(-)}(\xi; (q-1)h)$ at the sample points are given by

$$\tilde{\mathbf{a}}^{(i)} = \tilde{\mathbf{A}}^{(-)}\tilde{\boldsymbol{\psi}}^{(-)}(qh) + \tilde{\mathbf{A}}^{(+)}\tilde{\boldsymbol{\psi}}^{(+)}((q-1)h) \quad (15)$$

$$\tilde{\boldsymbol{\psi}}^{(+)}(qh) = \tilde{\mathbf{V}}\tilde{\boldsymbol{\psi}}^{(+)}((q-1)h) + \tilde{\mathbf{B}}^{(+)}\tilde{\mathbf{a}}^{(s)} \quad (16)$$

$$\tilde{\boldsymbol{\psi}}^{(-)}((q-1)h) = \tilde{\mathbf{V}}\tilde{\boldsymbol{\psi}}^{(-)}(qh) + \tilde{\mathbf{B}}^{(-)}\tilde{\mathbf{a}}^{(s)} \quad (17)$$

with

$$\tilde{\mathbf{a}}^{(f)} = \begin{pmatrix} \bar{\mathbf{a}}^{(f)}(\xi_1) \\ \vdots \\ \bar{\mathbf{a}}^{(f)}(\xi_L) \end{pmatrix}, \quad \tilde{\boldsymbol{\psi}}^{(\pm)}(y) = \begin{pmatrix} \bar{\boldsymbol{\psi}}^{(\pm)}(\xi_1, y) \\ \vdots \\ \bar{\boldsymbol{\psi}}^{(\pm)}(\xi_L, y) \end{pmatrix} \quad (18)$$

$$\tilde{\mathbf{A}}^{(\pm)} = \begin{pmatrix} \mathbf{A}^{(\pm)}(\xi_1)^t\mathbf{V}(h/2;\xi_1) & & \mathbf{0} \\ & \ddots & \\ \mathbf{0} & & \mathbf{A}^{(\pm)}(\xi_L)^t\mathbf{V}(h/2;\xi_L) \end{pmatrix} \quad (19)$$

$$\tilde{\mathbf{B}}^{(\pm)} = \begin{pmatrix} \mathbf{V}(h/2;\xi_1)\mathbf{B}^{(\pm)}(\xi_1)^t & & \mathbf{0} \\ & \ddots & \\ \mathbf{0} & & \mathbf{V}(h/2;\xi_L)\mathbf{B}^{(\pm)}(\xi_L)^t \end{pmatrix} \quad (20)$$

$$\tilde{\mathbf{V}} = \begin{pmatrix} \mathbf{V}(h;\xi_1) & & \mathbf{0} \\ & \ddots & \\ \mathbf{0} & & \mathbf{V}(h;\xi_L) \end{pmatrix} \quad (21)$$

for $f = i$, s.

An approximate relation between the expansion coefficient matrices $\tilde{\mathbf{a}}^{(s)}$ and $\tilde{\mathbf{a}}^{(i)}$ are provided by Ref. [19] in the following form:

$$\tilde{\mathbf{a}}^{(s)} = \tilde{\mathbf{M}}^{(q)^{-1}}\tilde{\mathbf{C}}^{(q)}\tilde{\mathbf{a}}^{(i)} \tag{22}$$

with

$$\tilde{\mathbf{M}}^{(q)} = \begin{pmatrix} \mathbf{M}^{(q)}_{1,1} & \cdots & \mathbf{M}^{(q)}_{1,L} \\ \vdots & \ddots & \vdots \\ \mathbf{M}^{(q)}_{L,1} & \cdots & \mathbf{M}^{(q)}_{L,L} \end{pmatrix} \tag{23}$$

$$\tilde{\mathbf{C}}^{(q)} = \begin{pmatrix} \mathbf{C}^{(q)}_{1,1} & \cdots & \mathbf{C}^{(q)}_{1,L} \\ \vdots & \ddots & \vdots \\ \mathbf{C}^{(q)}_{L,1} & \cdots & \mathbf{C}^{(q)}_{L,L} \end{pmatrix} \tag{24}$$

$$\mathbf{M}^{(q)}_{l,l'} = \delta_{l,l'}\mathbf{T}^{-1} - \mathbf{C}^{(q)}_{l,l'}\mathbf{L}(\xi_{l'}) \tag{25}$$

$$\mathbf{C}^{(q)}_{l,l'} = \left(\delta_{l,l'} - \frac{w_{l'}}{k_d}\sum_{n\in\mathscr{D}^{(q)}} e^{-ind(\xi_l-\xi_{l'})}\right)\mathbf{I} \tag{26}$$

$$\mathbf{L}(\xi) = \sum_{n\in\mathbb{Z}\setminus\{0\}} \mathbf{G}^{(H^{(1)})}(-nd,0)^t e^{ind\xi} \tag{27}$$

$$\left(\mathbf{G}^{(H^{(1)})}(x,y)\right)_{n,m} = H^{(1)}_{n-m}(k_s\rho(x,y))e^{i(n-m)\phi(x,y)} \tag{28}$$

where $\{w_l\}_{l=1}^{L}$ denote the weight factors determined by the appropriate numerical integration scheme to approximate integrals by using the integrands at sample points. The (n, m)th-components of the transition-matrix $\mathbf{T}$ are given by

$$(\mathbf{T})_{n,m} = \delta_{n,m}\frac{\zeta_s J_n(k_s a)J_n'(k_c a) - \zeta_c J_n'(k_s a)J_n(k_c a)}{\zeta_c H_n^{(1)\prime}(k_s a)J_n(k_c a) - \zeta_s H_n^{(1)}(k_s a)J_n'(k_c a)} \tag{29}$$

for the TM-polarization, and

$$(\mathbf{T})_{n,m} = \delta_{n,m}\frac{\zeta_c J_n(k_s a)J_n'(k_c a) - \zeta_s J_n'(k_s a)J_n(k_c a)}{\zeta_s H_n^{(1)\prime}(k_s a)J_n(k_c a) - \zeta_c H_n^{(1)}(k_s a)J_n'(k_c a)} \tag{30}$$

for the TE-polarization.

From Eqs. (15)–(17) and (22), we obtain the relation between the amplitudes of the incoming and the outgoing plane-waves as

$$\begin{pmatrix} \tilde{\boldsymbol{\psi}}^{(+)}(qh) \\ \tilde{\boldsymbol{\psi}}^{(-)}((q-1)h) \end{pmatrix} = \begin{pmatrix} \mathbf{S}^{(q)}_{11} & \mathbf{S}^{(q)}_{12} \\ \mathbf{S}^{(q)}_{21} & \mathbf{S}^{(q)}_{22} \end{pmatrix} \begin{pmatrix} \tilde{\boldsymbol{\psi}}^{(-)}(qh) \\ \tilde{\boldsymbol{\psi}}^{(+)}((q-1)h) \end{pmatrix} \tag{31}$$

where the submatrices of the S-matrix is given by

$$\mathbf{S}_{11}^{(q)} = \tilde{\mathbf{B}}^{(+)} \tilde{\mathbf{M}}^{(q)^{-1}} \tilde{\mathbf{C}}^{(q)} \tilde{\mathbf{A}}^{(-)} \tag{32}$$

$$\mathbf{S}_{12}^{(q)} = \tilde{\mathbf{B}}^{(+)} \tilde{\mathbf{M}}^{(q)^{-1}} \tilde{\mathbf{C}}^{(q)} \tilde{\mathbf{A}}^{(+)} + \tilde{\mathbf{V}} \tag{33}$$

$$\mathbf{S}_{21}^{(q)} = \tilde{\mathbf{B}}^{(-)} \tilde{\mathbf{M}}^{(q)^{-1}} \tilde{\mathbf{C}}^{(q)} \tilde{\mathbf{A}}^{(-)} + \tilde{\mathbf{V}} \tag{34}$$

$$\mathbf{S}_{22}^{(q)} = \tilde{\mathbf{B}}^{(-)} \tilde{\mathbf{M}}^{(q)^{-1}} \tilde{\mathbf{C}}^{(q)} \tilde{\mathbf{A}}^{(+)}. \tag{35}$$

This can be rewritten as a relation between the plane-wave amplitudes at $y = qh$ and $y = (q-1)h$ as

$$\begin{pmatrix} \tilde{\boldsymbol{\psi}}^{(+)}(qh) \\ \tilde{\boldsymbol{\psi}}^{(-)}(qh) \end{pmatrix} = \mathbf{F}^{(q)} \begin{pmatrix} \tilde{\boldsymbol{\psi}}^{(+)}((q-1)h) \\ \tilde{\boldsymbol{\psi}}^{(-)}((q-1)h) \end{pmatrix} \tag{36}$$

where the matrix $\mathbf{F}^{(q)}$ is the transfer matrix for the qth-layer and given as

$$\mathbf{F}^{(q)} = \begin{pmatrix} \mathbf{S}_{12}^{(q)} - \mathbf{S}_{11}^{(q)} \mathbf{S}_{21}^{(q)^{-1}} \mathbf{S}_{22}^{(q)} & \mathbf{S}_{11}^{(q)} \mathbf{S}_{21}^{(q)^{-1}} \\ -\mathbf{S}_{21}^{(q)^{-1}} \mathbf{S}_{22}^{(q)} & \mathbf{S}_{21}^{(q)^{-1}} \end{pmatrix}. \tag{37}$$

3.2. Floquet-modal Analysis

Let $\beta_n^{(q)}$ and $\boldsymbol{r}_n^{(q)}$ be the nth-eigenvalues and the associated eigenvectors of the transfer matrix $\mathbf{F}^{(q)}$, respectively. When implementing a practical computation, various infinite sums must be truncated. We denote the truncation order for the plane-wave expansion by N that truncates the expansion from $-N$th- to Nth-order. Then, the order of $\mathbf{F}^{(q)}$ is $2L(2N+1)$, and we arrange the $2L(2N+1)$ eigenvalues $\{\beta_n^{(q)}\}_{n=1}^{2L(2N+1)}$ in such a way that $\{\beta_n^{(q)}\}_{n=1}^{L(2N+1)}$ correspond to the Floquet-modes propagating in the positive y-direction and $\{\beta_n^{(q)}\}_{n=L(2N+1)+1}^{2L(2N+1)}$ correspond to the modes propagating in the negative y-direction. We classify the propagation directions of the Floquet-modes in the following rules:

- if $|\beta_n^{(q)}| < 1$, the corresponding mode is the evanescent one propagating in the positive y-direction.
- if $|\beta_n^{(q)}| > 1$, the corresponding mode is the evanescent one propagating in the negative y-direction.
- if $|\beta_n^{(q)}| = 1$, the corresponding mode is the guided one. When the modal power carried in the y-direction is positive (negative), the corresponding mode propagates in the positive (negative) y-direction.

Here we define column matrices $\mathbf{b}^{(q,+)}(y)$ and $\mathbf{b}^{(q,-)}(y)$ by

$$\begin{pmatrix} \mathbf{b}^{(q,+)}(y) \\ \mathbf{b}^{(q,-)}(y) \end{pmatrix} = \mathbf{R}^{(q)^{-1}} \begin{pmatrix} \boldsymbol{\psi}^{(+)}(y) \\ \boldsymbol{\psi}^{(-)}(y) \end{pmatrix} \tag{38}$$

with

$$\mathbf{R}^{(q)} = \left(\boldsymbol{r}_1^{(q)} \ldots \boldsymbol{r}_{4N+2}^{(q)} \right). \tag{39}$$

From Eqs. (36) and (38), we may understand that each component of $\mathbf{b}^{(q,\pm)}(qh)$ gives the amplitude of the Floquet-modes propagating in the $\pm y$-direction at $y = qh$. Also, the propagation constants of the nth-modes are given by

$$\eta_n^{(q)} = -i \frac{\mathrm{Ln}\left(\beta_n^{(q)}\right)}{h} \tag{40}$$

where Ln is the principal natural logarithm function.

3.3. Scattering-matrix for Composite Structure

The structure under consideration is thought as a cascade connection of straight PCW with different defects, in which the discontinuities are located at $y = qh$ ($q = 0, 1, \ldots, Q$), and the wave propagation can be formulated by the modal analysis. We define here the S-matrix for the region $0 < y < qh$ as

$$\begin{pmatrix} \mathbf{b}^{(0,-)}(0) \\ \mathbf{b}^{(q+1,+)}(qh) \end{pmatrix} = \begin{pmatrix} \mathbf{S}_{q,11} & \mathbf{S}_{q,12} \\ \mathbf{S}_{q,21} & \mathbf{S}_{q,22} \end{pmatrix} \begin{pmatrix} \mathbf{b}^{(0,+)}(0) \\ \mathbf{b}^{(q+1,-)}(qh) \end{pmatrix}. \tag{41}$$

The boundary conditions at $y = qh$ are given by equating the Fourier coefficients of tangential field components in both sides, and yield

$$\begin{pmatrix} \mathbf{b}^{(q+1,+)}(qh) \\ \mathbf{b}^{(q+1,-)}(qh) \end{pmatrix} = \begin{pmatrix} \mathbf{G}_{11}^{(q)} & \mathbf{G}_{12}^{(q)} \\ \mathbf{G}_{21}^{(q)} & \mathbf{G}_{22}^{(q)} \end{pmatrix} \begin{pmatrix} \mathbf{b}^{(q,+)}(qh) \\ \mathbf{b}^{(q,-)}(qh) \end{pmatrix} \tag{42}$$

with

$$\begin{pmatrix} \mathbf{G}_{11}^{(q)} & \mathbf{G}_{12}^{(q)} \\ \mathbf{G}_{21}^{(q)} & \mathbf{G}_{22}^{(q)} \end{pmatrix} = \mathbf{R}^{(q+1)^{-1}} \mathbf{R}^{(q)}. \tag{43}$$

Also, Eqs. (36) and (38) give the following relations:

$$\mathbf{b}^{(q,+)}(qh) = \mathbf{D}^{(q,+)} \mathbf{b}^{(q,+)}((q-1)h) \tag{44}$$

$$\mathbf{b}^{(q,-)}((q-1)h) = \mathbf{D}^{(q,-)} \mathbf{b}^{(q,-)}(qh) \tag{45}$$

$$\left(\mathbf{D}^{(q,+)}\right)_{n,m} = \delta_{n,m} e^{i\eta_n^{(q)} h} \tag{46}$$

$$\left(\mathbf{D}^{(q,-)}\right)_{n,m} = \delta_{n,m} e^{-i\eta_{L(2N+1)+n}^{(q)} h} \tag{47}$$

for n, $m = 0, 1, \ldots, L(2N+1)$.

From Eq. (42) for $q = 0$, the initial S-matrices are derived as follows:

$$\mathbf{S}_{0,12} = \mathbf{G}_{22}^{(0)^{-1}} \tag{48}$$

$$\mathbf{S}_{0,11} = -\mathbf{S}_{0,12}\mathbf{G}_{21}^{(0)} \tag{49}$$

$$\mathbf{S}_{0,21} = \mathbf{G}_{11}^{(0)} + \mathbf{G}_{12}^{(0)}\mathbf{S}_{0,11} \tag{50}$$

$$\mathbf{S}_{0,22} = \mathbf{G}_{12}^{(0)}\mathbf{S}_{0,12}. \tag{51}$$

When S-matrices $\mathbf{S}_{q-1,11}$, $\mathbf{S}_{q-1,12}$, $\mathbf{S}_{q-1,21}$, and $\mathbf{S}_{q-1,22}$ are given, S-matrices of the region $0 < y < q\,h$ are derived from Eqs. (42), (44), (45) as follows:

$$\mathbf{S}_{q,12} = \mathbf{S}_{q-1,12}\mathbf{D}^{(q)}\boldsymbol{W}_{q,1}{}^{-1} \tag{52}$$

$$\mathbf{S}_{q,11} = \mathbf{S}_{q-1,11} - \mathbf{S}_{q,12}\mathbf{G}_{21}^{(q)}\mathbf{D}^{(q)}\mathbf{S}_{q-1,21} \tag{53}$$

$$\mathbf{S}_{q,22} = \boldsymbol{W}_{q,2}\boldsymbol{W}_{q,1}{}^{-1} \tag{54}$$

$$\mathbf{S}_{q,21} = \left(\mathbf{G}_{11}^{(q)} - \mathbf{S}_{q,22}\mathbf{G}_{21}^{(q)}\right)\mathbf{D}^{(q)}\mathbf{S}_{q-1,21} \tag{55}$$

with

$$\boldsymbol{W}_{q,1} = \mathbf{G}_{22}^{(q)} + \mathbf{G}_{21}^{(q)}\mathbf{D}^{(q)}\mathbf{S}_{q-1,22}\mathbf{D}^{(q)} \tag{56}$$

$$\boldsymbol{W}_{q,2} = \mathbf{G}_{12}^{(q)} + \mathbf{G}_{11}^{(q)}\mathbf{D}^{(q)}\mathbf{S}_{q-1,22}\mathbf{D}^{(q)}. \tag{57}$$

Consequently, S-matrices $\mathbf{S}_{Q,11}$, $\mathbf{S}_{Q,12}$, $\mathbf{S}_{Q,21}$, and $\mathbf{S}_{Q,22}$ for the entire region are obtained by the initial matrices Eqs. (48)–(51) and the recursive relations Eqs. (52)–(57).

4. NUMERICAL EXPERIMENTS

To validate the present formulation, we show here some numerical results for specific examples. All the results are for the TM-polarized fields.

First, we consider the guided Floquet-modes propagating in coupled parallel PCWs schematically shown in Figure 2(a). The photonic crystal consists of cylinders with $\varepsilon_c = 11.56\,\varepsilon_0$, $\mu_c = \mu_0$, and $a = 0.2d$, and the surrounding medium is with $\varepsilon_s = \varepsilon_0$ and $\mu_s = \mu_0$. The wavelength in free space is $\lambda_0 = 1550\,\mathrm{nm}$ and the lattice constant is chosen as $d = h = 0.34\,\lambda_0$. This coupled PCWs support only two guided-modes. The method presented in Ref. [6] is known to provide highly accurate results for the guided-modes of the PCW

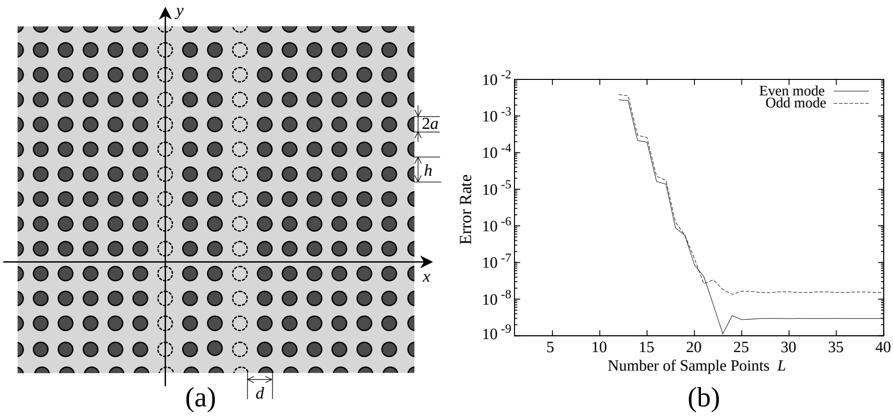

Figure 2. Coupled parallel photonic crystal waveguides. (a) Structure under consideration. (b) Convergence of the propagation constants.

formed by circular cylinders though it is not available for analyzing the evanescent-modes. We have performed the same computation with Ref. [6] and obtained accurate values as $2.34338750 \times 10^6\,\mathrm{m}^{-1}$ for the even guided-mode and $2.05692809 \times 10^6\,\mathrm{m}^{-1}$ for the odd one. We use these values as the reference ones. Figure 2(b) shows the error rates of the propagation constants of the guided-modes obtained by the present formulation as functions of the sampling point number. In this computation, the Brillouin zone is split at the Wood-Rayleigh anomalies, and the sample points and the weights are determined by applying the Gauss-Legendre scheme for the subintervals [19]. Also, the truncation orders for the plane-wave expansions N and for the cylindrical-wave expansions K are chosen for $N = 2$ and $K = 4$. Considering that the reference values are in nine-digit accuracy, the present formulation provides a fast convergence and the converged values are in good agreements with them.

Next, we show numerical results for some basic devices constructed by photonic crystal waveguides. the section $y < 0$ is supposed to consist of a single straight waveguide supporting only one guided Floquet-mode, and the fields are always excited from this side by the guided mode propagating in the positive y-direction. We choose the parameters for the surrounding photonic crystal as follows: permittivity of the surrounding medium $\varepsilon_s = \varepsilon_0$; lattice constants $d = h = 340\,\mathrm{nm}$; permittivity and radius of the arrayed cylinders $\varepsilon_c = 12.25\,\varepsilon_0$ and $a = 0.2\,d$; permeability of the surrounding medium and the arrayed cylinders $\mu_s = \mu_c = \mu_0$. Using these values, a waveguide formed by a single straight line defect supports only one guided

Floquet-mode and the fields are confined near the defects. Figure 3(a) shows a structure of photonic crystal waveguide filter consisting of a resonance cavity weakly coupled with straight waveguides. The transition section consists of five layers, in which the resonance cavity is formed by removing one cylinder in the third-layer, and the input/output sections are the single straight waveguides. The power reflection and transmission spectra of Figure 3(a) are computed for

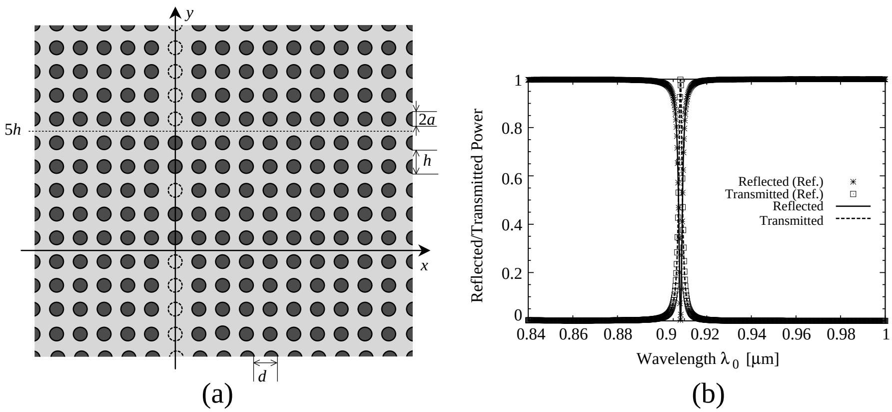

Figure 3. Photonic crystal waveguide filter consists of a resonance cavity weakly coupled with straight waveguides. (a) Structure under consideration. (b) Power reflection and transmission spectra.

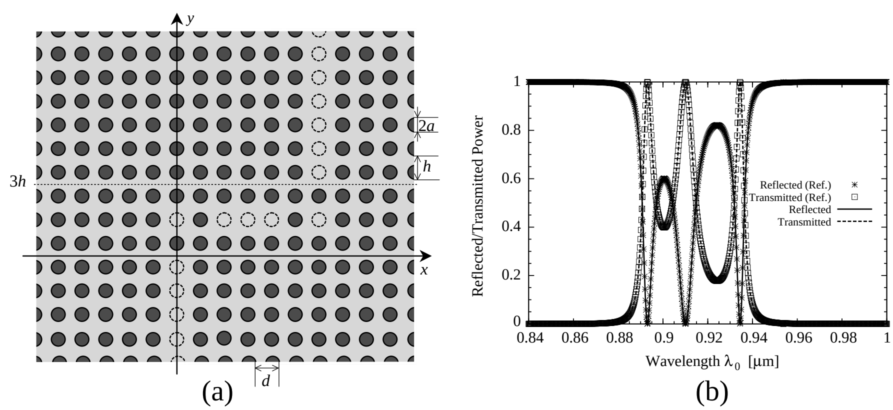

Figure 4. Photonic crystal crank with resonance cavities at the corners. (a) Structure under consideration. (b) Power reflection and transmission spectra.

$N = 2$, $K = 4$, and $L = 30$, and plotted in Figure 3(b). We also plotted the results obtained by the FSEM combined with the RTMA [16]. It is seen that the transmission spectra has sharp resonance peak at around $\lambda_0 = 0.91\,\mu\text{m}$, and the results of the present formulation are in very good agreement with those of the FSEM combined with the RTMA. Figure 4(a) shows a structure of photonic crystal crank with resonance cavities at the corners, and the obtained power spectra are shown in Figure 4(b). The transition section of this structure consists of three layers, and the input and the output waveguides do not face each other. We can see three resonance peaks as shown in Figure 4(b), and the results of the present formulation are in good agreement with the corresponding results of the formulation shown in Ref. [16].

5. CONCLUSION

This paper proposes a spectral-domain formulation of the pillar-type PCWD based on the RTMA with the use of the PPFT. The structure was treated as a multilayer structure of periodic circular cylinder arrays with defects, and the wave propagation was obtained by the modal analysis. The structure in each stacked layer is an imperfectly periodic due to the defects, and the fields have continuous spectra in the wavenumber space. To define the transfer matrix of stacked layer, we applied the PPFT, and the transformed fields were discretized in the Brillouin zone. Also, derivation of the transfer matrix was based on the RTMA with the lattice sums technique to accelerate the convergence. The Floquet-modes are obtained by the eigenvalue calculation of the transfer matrix, and the modal-analysis becomes possible without using periodic boundary conditions. The present formulation was validated by comparing with the numerical results with those of the conventional formulations. If the present formulation is applied to the photonic crystal of infinite extent without defects, the off-diagonal block elements of the matrices $\tilde{\mathbf{M}}^{(q)}$ and $\tilde{\mathbf{C}}^{(q)}$ are vanished and the formulation becomes completely same with the classical formulation of the RTMA with the lattice sums technique but with the use of wastefully large matrices.

REFERENCES

1. Koshiba, M., Y. Tsuji, and M. Hikari, "Time-domain beam propagation method and its application to photonic crystal circuits," *J. Lightwave Technol.*, Vol. 18, No. 1, 102–110, 2000.
2. Taflove, A., *Computational Electrodynamics: The Finite-difference Time-domain Method*, Artech House, Boston, 1995.

3. Benisty, H., "Modal analysis of optical guides with two-dimensional photonic band-gap boundaries," *J. Appl. Phys.*, Vol. 79, No. 10, 7483–7492, 1996.
4. Joannopoulos, J. D., R. D. Meade, and J. N. Winn, *Photonic Crystals: Molding the Flow of Light*, Princeton Univ. Press, Princeton, 1995.
5. Tanaka, H., T. Yamasaki, and T. Hosono, "Propagation characteristics of dielectric waveguides with slanted grating structure," *IEICE Trans. Electron.*, Vol. E77-C, No. 11, 1820–1827, 1994.
6. Yasumoto, K., H. Jia, and S. Kai, "Rigorous analysis of two-dimensional photonic crystal waveguides," *Proc. URSI Int. Symp. on Electromagnetic Theory*, 739–741, 2004.
7. Jia, H. and K. Yasumoto, "Modal analysis of two-dimensional photonic-crystal waveguides formed by rectangular cylinders using an improved Fourier series method," *IEEE Trans. Microwave Theory and Techniques*, Vol. 54, No. 2, 564–571, 2006.
8. Li, L., "Formulation and comparison of two recursive matrix algorithms for modeling layered diffraction gratings," *J. Opt. Soc. Am. A*, Vol. 13, No. 5, 1024–1035, 1996.
9. Hosono, T., T. Hinata, and A. Inoue, "Numerical analysis of the discontinuities in slab dielectric waveguides," *Radio Sci.*, Vol. 17, No. 1, 75–83, 1982.
10. Yamakita, J., K. Matsumoto, and K. Rokushima, "Analysis of discontinuities in anisotropic dielectric waveguides," IEICE Technical Report, EMT-93-87, 1993 (in Japanese).
11. Yasumoto, K., T. Miyamoto, and M. Momoda, "Full-wave analysis of optical waveguides using periodic boundary conditions," *Proc. SPIE*, Vol. 3666, 170–176, 1999.
12. Li, Z. Y. and K. M. Ho, "Light propagation in semi-infinite photonic crystal and related waveguide structures," *Physical Review B*, Vol. 68, 155101, 2003.
13. Watanabe, K. and K. Yasumoto, "Accuracy improvement of the Fourier series expansion method for Floquet-mode analysis of photonic crystal waveguides," *Progress In Electromagnetics Research*, Vol. 92, 209–222, 2009.
14. Yasumoto, K. and H. Toyama, "Formulation for electromagnetic scattering and guidance by two-dimensional photonic crystals," IEICE Technical Report, OPE2001-93, 2001.
15. Yasumoto, K. and K. Watanabe, "Analysis of discontinuities in two-dimensional photonic crystal waveguides using Floquet modes

concept," *Int. J. Microwave and Opt. Technol.*, Vol. 3, No. 3, 397–403, 2008.

16. Nakatake, Y. and K. Watanabe, "Numerical analysis of two-dimensional photonic crystal waveguide devices using periodic boundary conditions," *IEICE Trans. Electron.*, Vol. E94-C, No. 1, 32–38, 2011.
17. Chew, W. C., *Waves and Fields in Inhomogeneous Media*, Van Nostrand Reinhold, New York, 1990.
18. Watanabe, K. and K. Yasumoto, "Two-dimensional electromagnetic scattering of non-plane incident waves by periodic structures," *Progress In Electromagnetics Research*, Vol. 74, 241–271, 2007.
19. Watanabe, K., Y. Nakatake, and J. Pištora, "Accurate analysis of electromagnetic scattering from periodic circular cylinder array with defects," *Optics Express*, Vol. 20, No. 10, 10646–10657, 2012.